Modeling and Simulations of MEMS Gyroscope with Matlab/SIMULINK Package

Jacek Nazdrowicz

***Abstract*—This paper presents developed mathematical model of MEMS gyroscope created in Matlab/SIMULINK environment. The model can be very useful for calculating MEMS gyroscope geometrical parameters. These parameters play very significant role, because they have huge and direct impact on device response, performance and further possibilities of application. Results of simulations are presented in this article separately for drive and sense direction. In addition there are also results in frequency domain presented. With all these results we obtain quick overview of behavior this kind of MEMS device and response characteristics.**

***Index Terms*—MEMS, gyroscope, angular velocity sensor, microelectromechanical systems, model simulation, microaccelerometer, MATLAB, SIMULINK, MEMS modeling, equivalent circuit model.**

I. Introduction

ENORMOUS growth of MEMS (Micro Electro Mechanical Systems) market at the beginning this century was caused by almost infinite possibilities of application. These devices (mostly sensors and actuators) found wide area of applications in many devices the humans use every day. Commercialization of use these devices brought about intensively growth electronics industry. Many companies include in their products small MEMS sensors or actuators. This causes that in one small device becomes multifunctional portable box, what is very comfortable for end users and enforce miniaturization some features of from macro to micro world. Unfortunately, not all phenomena met in macro world can easily be transformed to micro world, the limitations especially appears when mechanical structure is very complex and response characteristics are different. Overcome difficulties during designing MEMS devices gives in result strong position in electronic sector and influences on economic positive results either company or customer with saving money giving low-cost, low-dimension and low-weight devices. These factors became foundations of intensive developing electronic industry.

Because population of potential customers of MEMS based devices is very large, this branch of industry is condemned to success, even though R&D costs are relatively large. Although population of potential customers is very large, and continuously grows - still we have to do with dominance demand over supply, and as we can see results of market research predictions – trend will be growing.

J. Nazdrowicz is with the Department of Microelectronics and Computer Science, Lodz University of Technology, Lodz, Poland (e-mail: jnazdrowicz@dmcs.pl).

By definition, MEMS sensors are miniaturized devices used to measure inertial forces and transform them using specialized ASICs to useable physical quantities (fig. 1). MEMS gyroscope is one type of such sensors allowing to detect angular motion and measure angular velocity. It can also give information about acceleration and location.

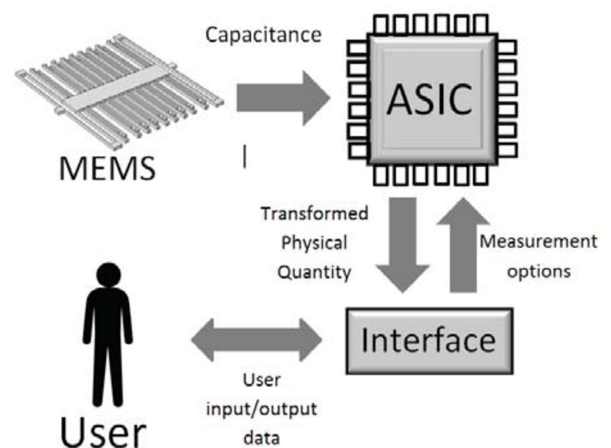

Fig. 1. Obtaining physical quantities from MEMS via ASIC.

The dimensions of MEMS devices are very small - in range of millimeters to micrometers. It is very important to take into account structural mechanics aspects and simplify geometry. Because of very small dimensions, importance existing forces is completely different from experience from these known in macro world. The good examples are inertia forces which are less important than damping and spring ones.

Small dimensions are requirements to use appropriate technology of manufacturing. Materials commonly used in Integrated Circuits (IC) manufacturing are greatly adaptable to micromechanisms, because of their physical and chemical properties. This allows to apply technology of preparation and manufacturing for these devices – the same like for Integrated Circuits. Additionally, common materials allow to manufacture these devices together with integrated circuits (processing the output signal from mechanical part), all on the same substrate; and all packaged in the same casing.

MEMS Gyroscopes are interesting area for researchers. Since 1978, when Friedland and Hutton [9] suggested the use of a vibratory gyroscope for measuring rotation quantities, many publications appeared related to this topic. Paper [5] includes useful widely-described mathematical foundations and principles for simulating microgyroscopes. Authors presented results of their simulations focused on analyzing the

ISSN 2080-8755 Copyright © 2017 by Department of Microelectronics & Computer Science, Lodz University of Technology

dynamic characteristics of vibratory microgyroaccelerometer. In publication [4] authors presented the design of MEMS gyroscope for high driving resonance frequency and analyzed device performance in dependency of different structural parameters. Behavioral model using electromechanical library in Simulink was presented in [6]. The model was, based on equations of motion, simulated by authors, and results were a subject of analyzing the frequency response and transient behavior of the device.

Microgyroscopes based on capacitive sensing principle are widely applied because they are characterized with high sensitivity, low level of noise, very high resolution, high performance, resistance on stresses and overloading – better parameters than met in piezoelectric, piezoresistive and thermal sensors [2].

It is obvious then, that area of research of MEMS sensors like gyroscopes is very complex and multidimensional, and we can observe growing interest of this kind of this group of devices.

II. Principle of Operation of MEMS Gyroscope

Fundamental equation showing behavior of MEMS gyroscope is motion equation which describes displacement under external force taking into consideration spring and damping forces. The equation has the following form:

$$ma = m\frac{d^2x}{dt^2} + b\frac{dx}{dt} + kx \tag{1}$$

As mentioned earlier MEMS gyroscope measures angular velocity ω. Principle of MEMS gyroscope operation is not complex. It uses Coriolis effect which appears in rotating objects (fig. 2).

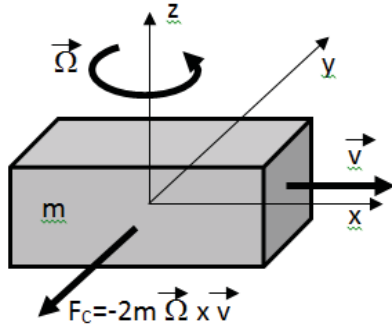

Fig. 2. Gyroscope operation principal.

When object rotates around z axis and additionally moves along axis which is orthogonal to rotating one (in this example x) additional force appears. Coriolis phenomena appears in rotating reference frames in MEMS gyroscopes. In case of clockwise rotation, force acts to the left of the motion of the object. In case of anticlockwise rotation, the force acts to the right direction. This is so called Coriolis force and equals[1,3]:

$$F_C = -2m(\vec{\Omega} \times \vec{v}) \tag{2}$$

where Ω is angular velocity, v – linear velocity, m – mass of object. The "minus" sign shows that force vector is opposite to motion direction. From this equation we see, that appearance of Coriolis force is conditioned by non-zero linear velocity with perpendicular direction to angular velocity axis.

Consequently in MEMS, this velocity needs to be enforced. MEMS gyroscope has two kind of motion: one is in driving direction (externally enforced) and one is in sense direction (fig. 3) – enforced by motion in drive direction.

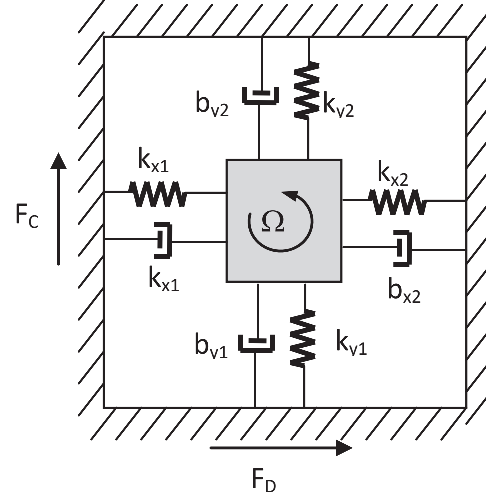

Fig. 3. MEMS gyroscope with spring and damping elements included operation principal (one cycle in one direction is presented).

Inertial mass hanging with springs, orthogonal located inside rotating frame additionally oscillates in *x* direction (tangential to rotating direction) (fig. 3). Motion in driving direction is enforced by actuator consist of comb structures [7] and located on opposite sides of devices along *x* direction. External force coming from this actuator has sinusoidal characteristics with constant period and amplitude. Obviously, proof mass vibrates also along *y* (sense) axis, where on opposite sides additional pair of comb drives is located. Motion of electrodes causes capacitance changes, what can be measured and transformed to other usable physical quantities (in this sensor – angular velocity). Consequently, it can be observed that this MEMS sensor is complex - includes cooperating sensor and actuator.

Because of these motions (in two orthogonal directions), two equations (1) governing this phenomena have been appropriately transformed. First one, describing motion in *x* (drive) direction is as following:

$$m\frac{d^2x}{dt^2} + b_x\frac{dx}{dt} + k_x x = F_D \sin(\omega t) \tag{3}$$

Second equation describes motion in *y* (sense) direction and includes Coriolis force and has a form:

$$m\frac{d^2y}{dt^2} + b_y\frac{dy}{dt} + k_y y = -2m\frac{dx}{dt}\Omega \tag{4}$$

where: m – vibrating mass, b_x, b_y – damping coefficient, k_x, k_y – spring coefficient, Ω – measured angular velocity, F_D – force generated by comb drive actuator.

Observe, that there is common factor of both equations (3) and (4) – *dx/dt* (linear velocity), which calculated from (3) needs to be substituted on right side of (4).

Looking at both equations we see, that there are some force components in both drive and sense directions – spring, damping and electrostatic forces which influence on motion characteristics. By design, electrostatic force in drive direction is source of necessary motion to enforce Coriolis Force in sense direction (F_D). For *y* (sense) direction, detection of capacitance requires electrodes to be loaded with appropriate voltage. This causes that additional force - electrostatic force is generated and should be considered on the right side of equation (4):

$$m\frac{d^2y}{dt^2}+b_y\frac{dy}{dt}+k_y y=-2m\frac{dx}{dt}\Omega+F_e \tag{5}$$

In fact, as it will be shown in simulation results – this electrostatic force can be very small, and in some case can be omitted because it does not meaningfully influence on response results.

All considered types of component forces can be calculated using following formulas:

$$F_b=b(x)\frac{dx}{dt}=\frac{\mu A^2}{2}\left[\frac{1}{(x_0-x)^3}+\frac{1}{(x_0+x)^3}\right]\frac{dx}{dt} \tag{6}$$

$$F_k=kx,\qquad F_e=\frac{\varepsilon_0 A}{4}\left(\frac{V_1^2}{(x_0-x)^2}-\frac{V_1^2}{(x_0+x)^2}\right) \tag{7}$$

where μ– air viscosity, V - voltage load, ε_o - permittivity coefficient, A – area of comb drive electrodes.

For sense direction equation will be analogous (*x* will be replaced with *y*).

III. MEMS Gyroscope Model Implementation in MATLAB/SIMULINK Environment

Model of MEMS gyroscope was implemented in Matlab/SIMULINK environment. It consists of two main parts: concerning with drive direction [7] and with sense direction. System is loaded with sinusoidal function force with amplitude of acceleration. Model also was tested with module including capacitances working in opposite phases to enforce as much as possible amplitude of motion. Sinusoidal generator has possibility input frequency what allows to create characteristics in frequency domain. In fig. 4. there is general schema of presented model with particular stages of calculations included.

Both drive and sensing parts of model have acceleration as an input and then two integrations are performed (in *x* and *y* direction separately). Model is very flexible, because it allows to input spring constants separately for both directions; also damping coefficients are calculated separately (this allows to adjust capacitor electrodes and spring dimensions for both directions of motion).

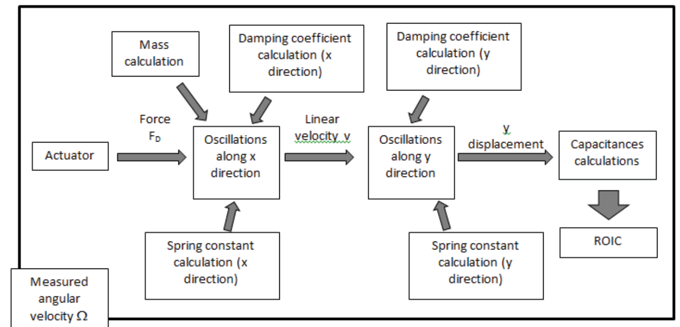

Fig. 4. General schema of the presented model.

The presented model is very complex and for convenience to use it was necessary to create functional subsystems within to clearly show what particular parts are responsible for (see also fig. 4). This has big advantage because it allows to update particular functional elements without any unnecessary influence to other parts. Moreover these subsystems can be easily replaced.

The general view of MEMS gyroscope Matlab/SIMULINK model includes value input boxes representing geometrical dimensions, material properties, drive load acceleration and measured value – angular velocity. Although model is very flexible, however it assumes that springs consist of straight beams. It can be very easily to transform to other kind of springs – it is necessary to add constant blocks and update function block with new calculation formula. General view of model is presented in fig. 5. Here it can be differentiate functional blocks – subsystems such as: *x* drive, *y* sense, mass calculation, spring constant calculation, forces calculation, *F* display preparation.

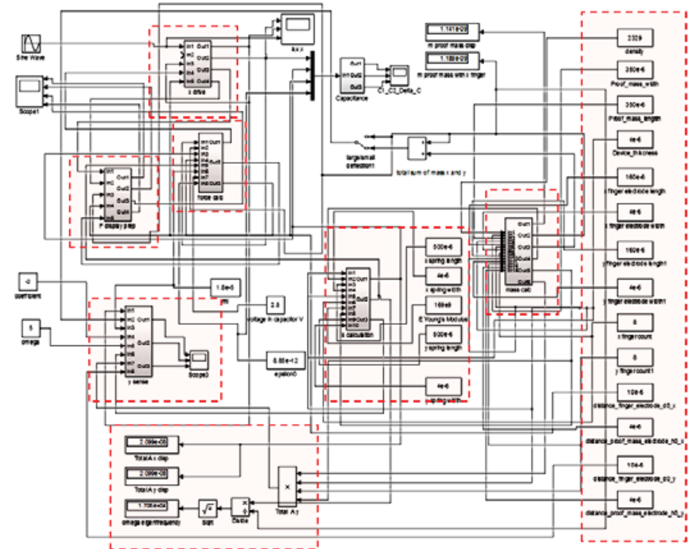

Fig. 5. General view of the model.

All of them have many inputs and output, and can be also used for other purposes. Below, these subsystems will be described.

x drive subsystem (fig. 6) is responsible for actuating using capacitance electrostatic force. This module implements first motion equation (3) and gives an output linear velocity and

displacement. The output velocity is necessary for second motion equation where the component of Coriolis Force exists. Displacement calculation is necessary to recalculate electrostatic force (distance between electrodes changes).

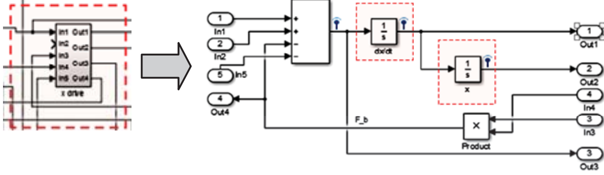

Fig. 6. Drive subsystem of model.

y sense subsystem (fig. 7) is very similar to X sense one, which implements equation (4). This subsystem takes as an input angular velocity (measured quantity) and linear velocity tangential to rotation coming from calculation made in X drive subsystem (right side of equation (4)).

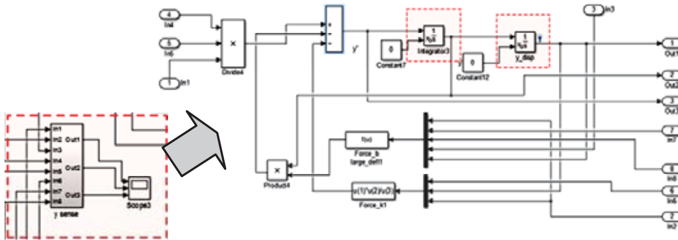

Fig. 7. Sense subsystem of model.

Force calculation (fig. 8) subsystem is responsible for calculation of particular component forces used in both (3) and (4) equations (separately): spring forces, damping forces and electrostatic forces. Electrostatic forces in drive direction (upper part of susbsystem) acts as the input force, in sense direction (bottom part of subsystem) acts as result additional electrostatic force generated by detecting system of electrodes.

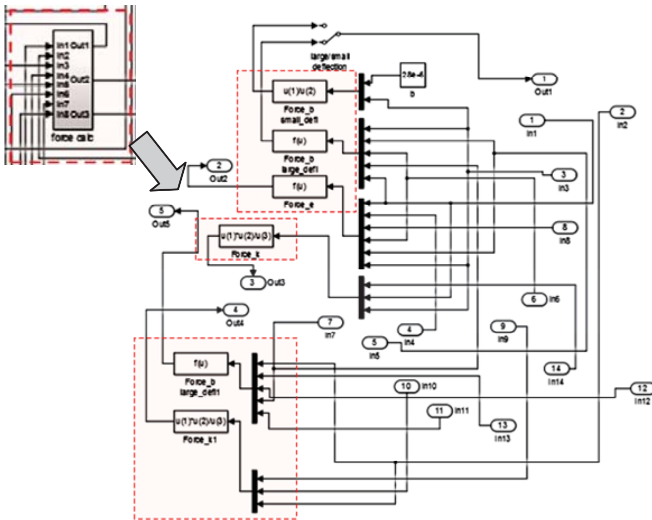

Fig. 8. x and y force calculation subsystem.

k calculation susbsystem is responsible for calculation spring constant based on geometry dimensions and formulas (7), (8) and (9). Spring constant is calculated separately for drive and sense directions using following formulas:

$$k_b = \frac{E \cdot w \cdot t^3}{4 \cdot L^3} \tag{7}$$

$$k_p = \sum_i k_{bi}, \frac{1}{k_s} = \sum_i \frac{1}{k_{bi}},$$

$$k_{tot} = \frac{k_b}{2} \tag{8}$$

Mass calculation subsystem (fig. 9) calculates particular components masses and creates sum of them for further use. The masses are calculated based on input geometrical dimensions (volumes calculation) and then multiplying by density. Output mass is not used on equation (3) and (4) only, but also for resonant frequency calculation based on equation:

$$\omega_0 = \sqrt{\frac{k_x}{m_x}} \tag{9}$$

x-indexes for k and m have key impact on ω_0 calculation; mass and spring calculation y quantities are intentionally omitted (mass of spring is very small in compare to total mass). However in this model there is possible to input total mass (for sense direction) of y mass component.

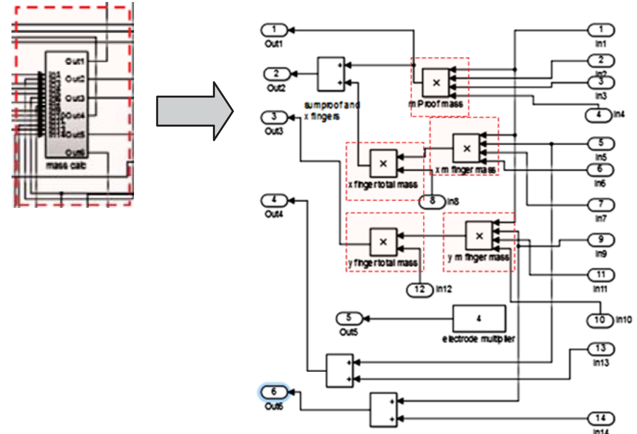

Fig. 9. Mass calculation subsystem.

Notice, that mass in x direction in fact should be smaller than in y direction (fig. 10). This difference is approximately equals mass of parts moving only along y direction (i.e. external springs). Although this model takes into consideration this factor, in case of small mass of springs compare to proof mass, total mass can be set the same for motion in x and y directions.

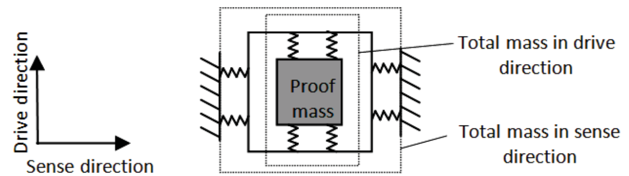

Fig. 10. Total mass for drive and sense direction.

Model was tested and no errors appeared. Moreover, simulations took results very quickly what is a big advantage, especially in so complex model with many functions calculated.

IV. Simulation Results of MEMS Gyroscope Simulink Model

Presented above model was loaded with geometric dimension and material properties data. Simulation time was 0.01s with variable step size between 10^{-6} and 10^{-5} with solver ode45. In table I there are constant parameters used in simulations.

TABLE I.
List of input parameters.

Symbol	Quantity	Value
μ	Air viscosity	$1.8\cdot10^{-5}$Ns/m^2
V	Voltage load	2.5V
ε_o	Permittivity coefficient	$8.854\cdot10^{12}$F/m,
ρ	Density (Polysilicon)	2328 kg/m^3
a	Acceleration	1g

Because of small dimensions of device, there are small deflections of spring which influence directly on capacitance sensing value. As the value is very small, it is difficult to detect this capacitance. It is important to take into account that displacement driven in x direction causes displacement in sense direction y which is some orders less (what will be later shown based on simulation results). On the other way geometrical dimensions, low voltage loaded capacitor and spring properties of material meaningfully limit possibility to enlarge range of displacement in drive direction. Enlarging this require requires to enlarge electrodes length, what as a result exposes electrodes to larger risk of short circuit and finally degrade of drive capacitor.

Other way to get better detection parameters is to use physical property of the material. Each one has its own characteristic frequency what depends on spring constant k and mass m (this is presented in formula (8)). Resonance phenomena ($\omega=\omega_0$) causes enormously large displacement. Knowing that frequency of oscillation in sense direction is the same as in drive direction, it suffices to set frequency of enforced vibrations equally to resonant frequency. It should cause increase amplitude of oscillations in sense directions. This phenomena was also simulated.

Tests were performed with external force causes sinusoidal acceleration a=1g. Model geometrical dimensions are placed in table II.

TABLE II.
List of geometrical parameters used in simulation.

Symbol	Quantity	Value
W_{el}	Static electrode width	$4\cdot10^{-6}$m
L_{el}	Static electrode length	$160\cdot10^{-6}$m
d_0	Initial distance between electrodes	$4\cdot10^{-6}$m
L_{spr}	Spring length	$500\cdot10^{-6}$m
W_m	proof mass width	$150\text{-}450\cdot10^{-6}$m
L_m	Proof mass length	$150\text{-}450\cdot10^{-6}$m
t	Device thickness	$4\cdot10^{-6}$m
W_f	Movable electrode width	$4\cdot10^{-6}$m
L_f	Movable electrode length	$160\cdot10^{-6}$m

First simulations of model were concerned with amplitude of oscillations with dependency on their frequency to verify oscillations along x axis (fig. 11). Tests were made for 2000Hz, 10000Hz and 20000Hz input (drive) frequency. Results of displacements of comb drive fingers in x direction are presented in fig. 10. Results of simulations show that there is very short period of time to stabilize oscillation amplitude and frequency influences on output x amplitude what is caused by inertia of proof mass. In conclusion - to get required amplitude fast, mass should be low weight. On the other side motion enforced by rotation with additional linear oscillation has low amplitude which depends also on inertia; in results - small deflections, as it mentioned earlier, are very difficult to detect and consequently in extreme cases – totally useless.

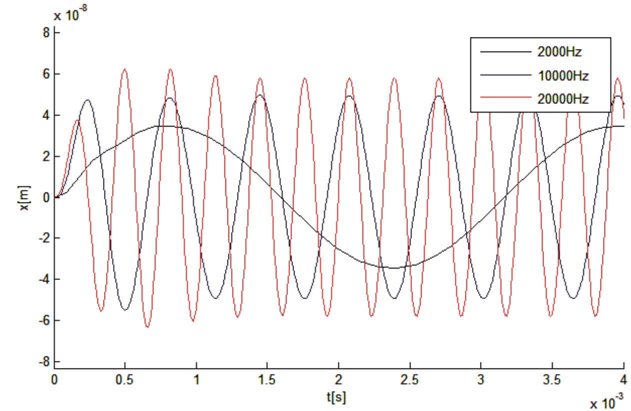

Fig. 11. Displacement dependency on input frequency in drive mode.

Next simulations were concerned with influence drive on sense motion in frequency domain (fig. 12). This is important, because it allows to adjust optimal oscillations of external force source. Performing these tests requires to compute spring coefficient, mass and then resonant frequency using equation (7), (8) and (9). Results were as following (for example for W_m=$450\cdot10^{-6}$m, L_m=$450\cdot10^{-6}$m): k=0.3461N/m, m=$1.189\cdot10^{-9}$m, ω_0=17060 1/s (results for other dimensions are presented in table III). Tests were performed for angular velocity Ω=5rad/s. Results of simulations in frequency domain shows that in case of resonance (calculated ω_0 is applied as external frequency of force source) there is dramatically growth of amplitude in y direction. Simulation results in fig. 12 are for different proof mass dimensions. As it can be seen, geometrical dimensions (especially mass, which is dominant part of total mass) have meaningful impact of characteristics in frequency domain.

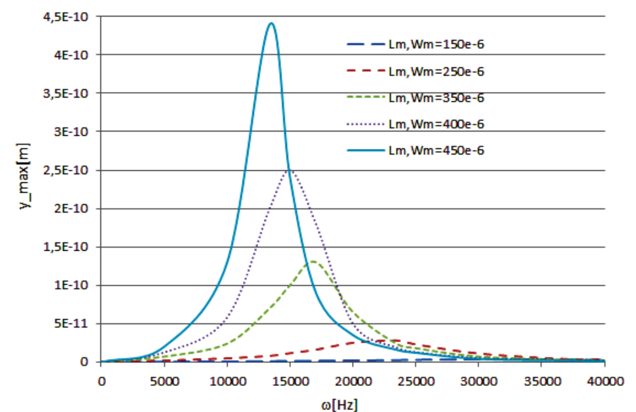

Fig. 12. Results of the simulations for geometry based on dimensions from table II.

Simulation confirms that large size of proof mass (L_m=450·10^{-6}m) gives much better results of y displacement than in small size case (L_m=250·10^{-6}m). Together with mass growth, resonant frequency drops and amplitude in resonant frequency enormously grows. For high resonant frequencies however, characteristics become more smooth. For large mass to get the best result (amplitude), frequency must be precisely fit (because characteristic is very steep and this way very sensitive on frequency changes). In table III there are calculated resonant frequencies for different proof mass dimensions.

TABLE III.
CALCULATED RESONANT FREQUENCIES FOR DIFFERENT DIMENSIONS.

W_m, L_m	ω_0
150·10^{-6}m	36680Hz
250·10^{-6}m	23440Hz
350·10^{-6}m	17060Hz
400·10^{-6}m	15000Hz
450·10^{-6}m	13380Hz

In fig. 13 there is displacement dependency in sense direction in case three different frequencies applied. One of these frequency is 13380Hz for W_m, L_m=450·10^{-6}m. One remaining frequency (10000Hz) is below resonant frequency and the other one is above (20000Hz). For resonant frequency one can see that displacement in y direction is much larger compared to other frequencies applied. In case of frequency other than resonant effective initial measuring time offset is about 2ms, because of vibrations with unpredictable amplitude. In case of resonant frequency this time enlarges to 3.2ms. For 20000Hz we see that maximum amplitude before measurement initial time can potentially be two times lower than in case of 10000Hz and two five times less than for resonant frequency. Notice, that because of unpredictable nature of amplitudes, for different frequencies they can be much higher than in these two characteristics.

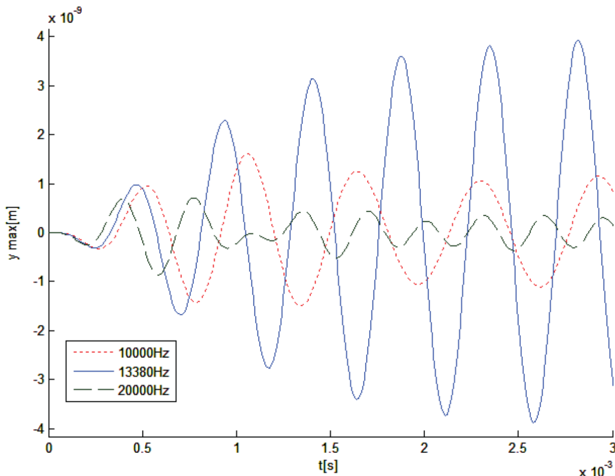

Fig. 13. Displacement dependency in sense direction for different frequency applied (including resonance frequency).

It is worth to analyze how device behave below and above resonant frequency of applied force. |This is clue because it allows to exclude unexpected effects during geometry design.

In case external force frequency, much higher or lower than resonant frequency (fig. 13 and 14), irregular fluctuation of amplitude appears at the beginning period of time. Then amplitude stabilizes, but not as good as in resonant frequency case. In stabilized amplitude phase there are small differences of maximum/minimum displacement, which should be taken into account during designing ReadOut Integrated Circuit.

Situation for lower frequencies is presented in fig. 14 and for higher frequencies – in fig. 15. Observing fig. 14 it can be seen that stabilization phase (lasts very shortly – and depends on frequency in fact) has potentially destructive impact on part of sense direction, because can lead to short circuit and damage sense capacitor. Moreover, it dramatically lessen device resolution because taking into consideration maximum amplitude that can be achieved in the stabilization phase and next relating to amplitude in stabilized phase (two times less in this case) it is obvious that half of whole possible displacement cannot be used for sense. As it mentioned before, stabilization phase lasts very shortly – but irregularities in sense y directions, exclude measure process in this time. That is why it is not effective solution. Otherwise, taking into account fact that measured capacitances in sense directions are very small and difficult to detect it is obvious that the best solution is to achieve maximum displacement as much as it is possible. Therefore, the optimized design should work in frequency close to or equals to resonant frequency.

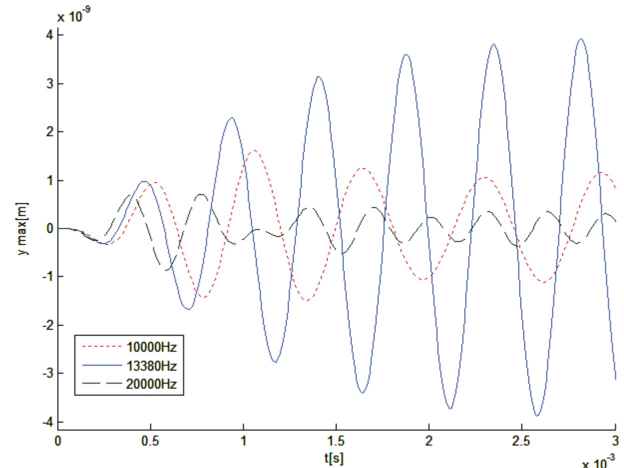

Fig. 13. Displacement dependency in sense direction for different frequency applied (including resonance frequency).

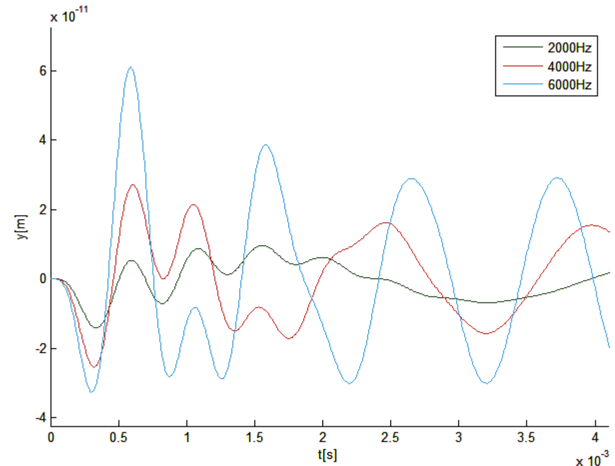

Fig. 14. Displacement dependency in sense direction for different frequency applied (below resonance frequency).

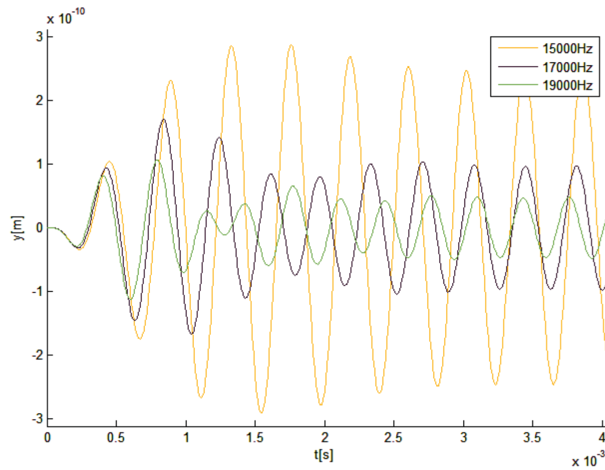

Fig. 15. Displacement dependency in sense direction for different frequency applied (above resonance frequency).

Fig. 16. shows comparison of forces acting on microgyroscope. Obviously, force related to acceleration F_a has highest amplitude than others (that is why displacement of proof mass takes place). The absolute sum of F_k and F_b in specified time grows hyperbolically and after amplitude stabilizes – becomes constant. The smallest importance has electrostatic force F_e, what can be omitted in this case.

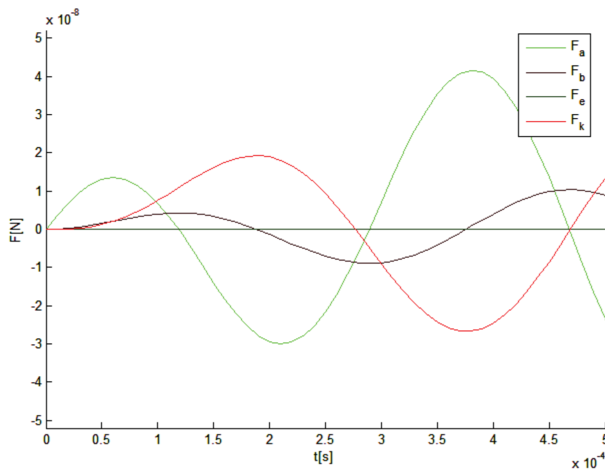

Fig. 16. Comparison of forces acting on microgyroscope. F_a – force related to acceleration, F_b – damping force, F_e – electrostatic force, F_k – spring force.

In fig. 17 there are calculated capacitances based on y displacement results (fig. 18). As we can see these are very small (10^{14} order). For other frequencies than resonant these capacitances are meaningfully smaller. For better precision difference between C_1 and C_2 is measured which has non-zero amplitude, because these characteristics are in opposite phase. However difference value is relatively small in compare to component capacitances.

In fig. 19. there are x and y maximum displacement characteristics compared in frequency domain.

From what one can see, both of them are non-linear. Along with frequency growth amplitudes decreases and for 36680Hz are almost 100 times less than for 9321Hz in case of x oscillations and almost 1000 times less in case of y oscillations. It should seek to fit geometry parameters to get resonant frequency as low as possible. This way it can obtain higher displacement in sense direction.

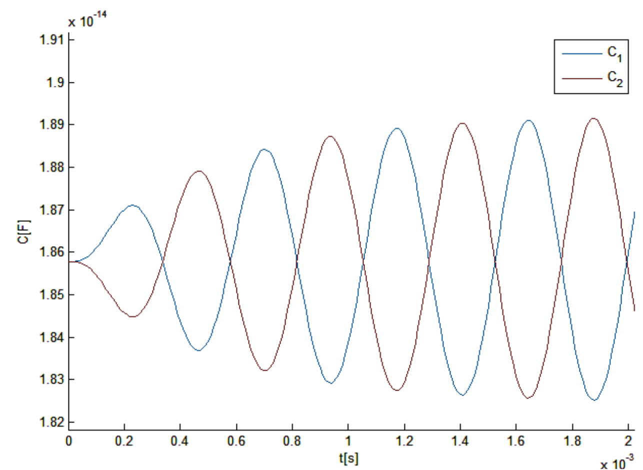

Fig. 17. Capacitances C_1 and C_2 resonant frequency applied for L_m=450·10^{-6}m.

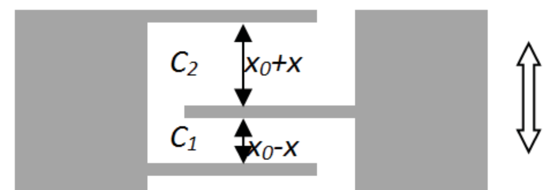

Fig. 18. Differences between capacitances C_1 and C_2 in comb drive structure.

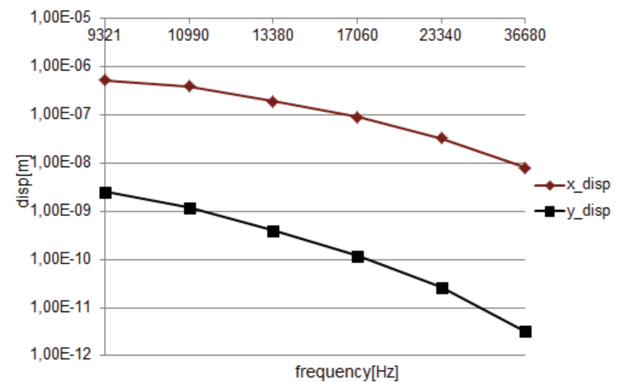

Fig. 19. Displacement characteristics in drive and sense directions for data in table IV.

TABLE IV.
CALCULATED DISPLACEMENTS IN DRIVE AND SENSE DIRECTIONS FOR DIFFERENT EIGENFREQENCIES

Frequency [Hz]	Displacement in drive direction [m]	Displacement in sense direction [m]
9321	5.20·10^{-7}	2.50·10^{-9}
10990	3.90·10^{-7}	1.20·10^{-9}
13380	1.90·10^{-7}	4.00·10^{-10}
17060	9.00·10^{-8}	1.20·10^{-10}
23340	3.30·10^{-8}	2.60·10^{-11}
36680	8.00·10^{-9}	3.20·10^{-12}

So far, frequency domain gyroscope behavior was analyzed. After performing simulations, it turned out that oscillations along the time are also interested. Analyze of these characteristics shows that two main phases can be differentiated – stabilization of oscillations and stabilized oscillations. Both phases have different characteristics depending on force frequency in drive direction. One way and the other phase of oscillation stabilization is less usable because it is not related to angular velocity itself.

CONCLUSIONS

In this article model of MEMS Gyroscope created in Matlab/SIMULINK was used. One can parametrize many options, including geometry, what allows simulate MEMS gyroscope with geometry details. It can reflect almost real shapes, what results will be more exact. Another advantage is that simulations takes less time than in case of Finite Element Analysis software.

Results of simulations shows very strong dependency between drive and sense directions. However small amplitude in *y* direction and small capacitance changes in result require to optimize geometry dimensions and apply appropriate frequency. It is important to emphasize, that resonant frequencies, which can give the best results of *y* displacement, should take into consideration, especially total mass of all parts of microgyroscope and spring constant in sense direction.

Results shows also that on mechanical point of view the most favorable geometry is that with large mass and relatively low frequency applied (equals resonant frequency), because it gives higher values of amplitude, and also capacitances.

Future works will concern with creation of equivalent electrical circuit model in Matlab/SIMULINK environment and comparison results to FEM model.

REFERENCES

[1] N. Yazdi et al., Micromachined inertial sensors, Proceedings of the IEEE, vol. 86, pp. 1640-1659, 1998.

[2] J. Wu, G.K. Fedder, L.R. Carley, A low-noise low-oflset capacitive sensing amplifier for a 50-/spl mu/g//spl radic/Hz monolithic CMOS MEMS accelerometer, IEEE of Solid-State Circuits, vol. 39, pp. 722-730, May 2004.

[3] C. Liu, Foundations of MEMS, Pearson Education Limited, India, 2012.

[4] P. Singh, P. Gupta, P. Srivastava, R. Kumari Chaudhary, Design and modeling of MEMS capacitive gyroscope, International Conference on Energy Efficient Technologies for Sustainability, Nagercoil, India, pp. 907-911, 10-12 April 2013.

[5] P. Verma, R. Gopal, S. Kumar Arya, Dynamic Characteristics of Vibratory Gyro-accelerometer, 5th International Conference on Computers and Devices for Communication (CODEC), Kolkata, India,17-19 Dec. 2012.

[6] P. Verma, R. Gopal, Arya , Sandeep K., Behavioral Simulation of a Non-resonant MEMS, Gyro-accelerometer, International Journal of Computer & Organization Trends, Volume 5, pp. 23-25, February 2014.

[7] W. Geiger, W. U. Butt, A. Gaisser. J. Frech, M. Braxmaier, T . Link, A. Kohne, P . Nommenson, H. Sandmaier, W. Lang, Decoupled Micro Gyros and the Design Principle DAVED, Sensors & Actuators A: Physical., vol. 95, no. 2-3, pp. 239- 249, 2002.

[8] X. Z . Chi., Z. Y. Guo, Z. C. Yang, L. T. Lin, Q. C. Zhao, J . Cui. G. Z. Yan, Decoupled Comb Capacitors for Microelectromechanical Tuning-Fork, Gyroscopes, IEEE Electron Devices, vol. 31, no. 1, 2010.

[9] B. Friedland, M. Hutton, Theory and error analysis of vibrating-member gyroscopes, IEEE Trans. Autom. Control 23 (4), pp. 545–556, 1978.

Jacek Nazdrowicz was born in Poddębice, Poland, in 1975. He received the MSc degrees in Technical Physics (Computer Physics), Computer Sciences (Software Engineering and Networking Systems) and Marketing and Management from the Lodz University of Technology, Poland, in 1999, 2000 and 2001 respectively and the PhD degree in Economics Sciences, Management discipline, in Lodz University of Technology, in 2013.
From 2014 he attends doctoral study in Lodz University of Technology, electronics discipline. His research interests include modelling and simulation MEMS devices and their application in medicine. He participated in EduMEMS project (Developing Multidomain MEMS Models for Educational Purposes). He also educates in COMSOL software. Now he participates in Strategmed project (supported by the National Center for Research and Development)
Between 2007 and 2016 he worked in mBank as a System Engineer of SQL Server databases. He has the following certifications: MCSA Windows 2012, MS SQL Server 2012 and Storage Area Network (SAN) Specialist.
Since 2016 he also works in Fujitsu Technology Solutions in Lodz in Remote Infrastructure Management Department in Storage Team as a Storage Engineer (SAN Infastructure, Brocade, Netapp, Eternus products). He educates in many data storage and backup technologies (IBM, DELL/EMC, Hitachi, Fujitsu).